OPEN ACCESS
CellPress

Cell Reports
Report

Appropriate Crypt Formation in the Uterus for Embryo Homing and Implantation Requires Wnt5a-ROR Signaling

Jeeyeon Cha,[1,2] Amanda Bartos,[1] Craig Park,[1] Xiaofei Sun,[1] Yingju Li,[1] Sang-Wook Cha,[2] Rieko Ajima,[3,4] Hsin-Yi Henry Ho,[5,6] Terry P. Yamaguchi,[3] and Sudhansu K. Dey[1,2,*]
[1]Division of Reproductive Sciences, Cincinnati Children's Hospital Medical Center, Cincinnati, OH 45229, USA
[2]Division of Developmental Biology, Cincinnati Children's Hospital Medical Center, Cincinnati, OH 45229, USA
[3]Cancer and Developmental Biology Laboratory, Center for Cancer Research, National Cancer Institute at Frederick, National Institutes of Health, Frederick, MD 21702, USA
[4]Division of Mammalian Development, National Institute of Genetics, Yata 1111, Mishima 411-8540, Japan
[5]Department of Neurobiology, Harvard Medical School, Boston, MA 02115, USA
[6]Department of Cell Biology and Human Anatomy, University of California Davis School of Medicine, Davis, CA 95616, USA
*Correspondence: sk.dey@cchmc.org
http://dx.doi.org/10.1016/j.celrep.2014.06.027

SUMMARY

Embryo homing and implantation occur within a crypt (implantation chamber) at the antimesometrial (AM) pole along the uterus. The mechanism by which this is achieved is not known. Here, we show that villi-like epithelial projections from the main uterine lumen toward the AM pole at regularly spaced intervals that form crypts for embryo implantation were disrupted in mice with uterine loss or gain of function of *Wnt5a*, or loss of function of both *Ror1* and *Ror2*. This disruption of Wnt5a-ROR signaling resulted in disorderly epithelial projections, crypt formation, embryo spacing, and impaired implantation. These early disturbances under abnormal Wnt5a-ROR signaling were reflected in adverse late pregnancy events, including defective decidualization and placentation, ultimately leading to compromised pregnancy outcomes. This study presents deeper insight regarding the formation of organized epithelial projections for crypt formation and embryo implantation for pregnancy success.

INTRODUCTION

Reciprocal interactions between the receptive uterus and blastocyst are critical to implantation. The uterus undergoes morphological, cellular, and molecular changes during pregnancy. This plasticity is reflected in its requirement for transcription factors, homeotic proteins, growth factors, morphogens, and signaling molecules (Cha et al., 2012). Genetic intervention of these signaling pathways results in defective or deferred implantation, which propagates adverse ripple effects throughout the remainder of gestation, compromising pregnancy success (Song et al., 2002; Ye et al., 2005; Sun et al., 2012).

Blood vessels enter the uterus through the mesometrium, positioning the uterus along a mesometrial-antimesometrial (M-AM) axis. Normally, implantation occurs within a crypt (implantation chamber) at the AM pole, as evident from histology of uterine cross-sections (Daikoku et al., 2011). Blastocyst attachment to the luminal epithelium (LE) occurs in the evening of day 4 of pregnancy (18:00–20:00 hr) and is coincident with increased endometrial vascular permeability at the site of blastocyst attachment. In mice, this vascular permeability can be monitored by intravenous injection of a blue dye solution, which marks the implantation sites (ISs) as distinct blue bands (Psychoyos, 1973). With progression of implantation on day 5, stromal cells around the implantation chamber undergo proliferation and differentiation into specialized decidual cells (decidualization). Decidualization supports embryonic growth and development and later directs placentation to establish maternal-fetal vascular connection.

Wnt signaling is a conserved pathway with roles in organogenesis and cell fate determination (Angers and Moon, 2009; MacDonald et al., 2009; van Amerongen and Nusse, 2009). In canonical signaling, Wnt ligands bind Frizzled (Fzd) and LRP5/LRP6 receptors to stabilize β-catenin for nuclear translocation; β-catenin then binds to T cell factor/lymphoid enhancer-binding factor and activates gene transcription. In noncanonical signaling, Wnts function independently of β-catenin-mediated transcription to direct cell movements, cell shape, and polarity (Kikuchi et al., 2011; van Amerongen and Nusse, 2009; Veeman et al., 2003). Wnt5a is considered a noncanonical Wnt ligand, and *Wnt5a* deletion in *Xenopus*, zebrafish, and mice disturbs directed cellular movements and polarity (Gao et al., 2011; Miyoshi et al., 2012; Schambony and Wedlich, 2007; Yamaguchi et al., 1999).

Several receptors including Fzd, ROR, and Ryk were shown to mediate noncanonical Wnt5a signaling in various systems (Green et al., 2008; Macheda et al., 2012; Minami et al., 2010; Niehrs, 2012). Significance of Wnt5a-ROR signaling in morphogenetic movement was recently reported in mouse embryogenesis (Ho et al., 2012). However, its role in the adult female reproductive tract during pregnancy is unknown.

Utilizing the *LoxP-Cre* system, we show here that an appropriate dosage of Wnt5a is required for normal blastocyst attachment and implantation. Females with either uterine inactivation (*Wnt5a*$^{d/d}$) or overexpression (*Wnt5a*^{GOF}) of *Wnt5a* are sterile or give birth to small litters. This subfertility phenotype is due to aberrant blastocyst attachment arising from defective LE organization, crypt formation, and embryo positioning in the uterus. These aberrations led to defective implantation, embryo crowding, poor decidualization, and placentation, leading to increased resorption rate and subfertility. Mice with uterine inactivation of both *Ror1* and *Ror2* (*Ror1*$^{d/d}$/*Ror2*$^{d/d}$) also showed similar phenotypes. These results suggest that uterine Wnt5a-ROR signaling contributes to appropriate uterine LE organization and crypt formation for blastocyst attachment.

RESULTS

Wnt5a Is Expressed in a Spatiotemporal Manner in the Peri-implantation Uterus

To better understand the function of Wnt5a in early pregnancy, we assessed the spatiotemporal uterine *Wnt5a* expression. Although *Wnt5a* expression was low to undetectable on days 1 and 2 of pregnancy, the expression was localized to the LE and subepithelial stroma on days 3 and 4, prior to and during the receptive phase. With implantation, the expression was highly localized in stromal cells at the M pole on day 5 (Figure 1A). On day 8, uterine *Wnt5a* expression was lower, indicating downregulation with pregnancy progression (Figure 1A). These results suggest that whereas *Wnt5a* expression on days 3 and 4 is associated with uterine receptivity, its localized expression at the M pole on day 5 shows a Wnt5a gradient along the M-AM axis.

Mice with Uterine Inactivation of *Wnt5a* Show Severely Compromised Fertility

To explore uterine Wnt5a's role in pregnancy, we generated females with uterine inactivation of *Wnt5a* (*Wnt5a*$^{d/d}$). *Wnt5a*$^{d/d}$ females and their floxed littermates (*Wnt5a*$^{f/f}$) were mated with wild-type (WT) males. We found that >70% of plug-positive *Wnt5a*$^{d/d}$ females failed to produce any litters after multiple matings (Figure 1B). Moreover, those 33% of plug-positive *Wnt5a*$^{d/d}$ females that delivered pups had significantly small litter sizes (Figure 1B). Females with deletion of one allele of *Wnt5a* showed a modest reduction in litter size: *Wnt5a*$^{d/+}$, 5.0 ± 1.4 pups/litter (n = 4); *Wnt5a*$^{f/f}$, 8.0 ± 0.6 (n = 6; mean ± SEM). This suggests that regulated Wnt5a levels are critical for pregnancy success. Wnt5a was efficiently deleted in *Wnt5a*$^{d/d}$ uteri, but not completely absent on days 4 or 5 of pregnancy (Figures 1C and 1D). The residual Wnt5a may explain retention of some fertility in *Wnt5a*$^{d/d}$ females.

Mice with Uterine Overexpression of *Wnt5a* Show Reduced Fertility

To further assess Wnt5a's role, we generated females with uterine overexpression of *Wnt5a* (*Wnt5a*^{GOF}) (Figures S1A–S1E). *Wnt5a*^{GOF} females mated with WT males had a significant reduction in litter size (Figure 1B). We confirmed upregulation of *Wnt5a* in *Wnt5a*^{GOF} uteri on the mornings of days 4 and 5. In situ hybridization results showed ectopic *Wnt5a* expression in all major uterine compartments (Figure 1C), and Wnt5a protein levels were 2- to 3-fold higher in *Wnt5a*^{GOF} uteri (Figure 1D). Interestingly, females with one allele of overexpressed *Wnt5a* showed normal litter size: Wnt5a$^{GOF/+}$, 7.0 ± 1.4 pups/litter; *Wnt5a*$^{f/f}$, 8.3 ± 1.3 (n = 5; mean ± SEM).

Approaching blastocyst attachment, the receptive uterine LE shows a decrease in apicobasal cell polarity with the loss of surface microvilli to facilitate trophectoderm adhesion to the apical surface of the LE (Daikoku et al., 2011; Schlafke and Enders, 1975). Electron microscopy (EM) analysis showed persistent apicobasal polarity of the LE in *Wnt5a*$^{d/d}$ and *Wnt5a*^{GOF} mice with higher cell heights and retention of glycosylated microvilli on the apical surface (Figure 1E). These results suggest that aberrant uterine Wnt5a levels interfered with critical aspects of the attachment reaction.

Wnt5a$^{d/d}$ and *Wnt5a*^{GOF} Mice Show Defective Implantation

To address the severe subfertility phenotypes in *Wnt5a*$^{d/d}$ and *Wnt5a*^{GOF} females, we examined implantation status on day 5 of pregnancy. We found that *Wnt5a*$^{d/d}$ or *Wnt5a*^{GOF} uteri either failed to show blue bands or had very weak bands compared to those in floxed littermates (Figure 1F), and unattached blastocysts were recovered from their uteri. In addition, ISs in these females were often irregularly spaced (Figure 1F). These characteristics were reflected in cross-sections of day 5 ISs with embryo implantation in the middle of the lumen (Figure S1F). We next asked whether decidualization and continued embryonic growth are affected under aberrant Wnt5a signaling.

Decidual Development Is Aberrant in Females with Dysregulated Uterine Wnt5a Levels

In mice, stromal cells surrounding the blastocyst undergo differentiation to form the primary decidual zone (PDZ) beginning in the afternoon on day 5. The PDZ is avascular with stromal cells assuming organized epithelioid characteristics with the acquisition of epithelial cell markers (Paria et al., 1999). The presumed functions of the PDZ are to support the early developing embryo and protect it from noxious substances from the maternal circulation by creating a selective barrier (Paria et al., 1999). By day 6, the PDZ is well developed, and a secondary decidual zone (SDZ) begins to form at the periphery of the PDZ. Decidual growth peaks between days 7 and 8, after which the decidua progressively regresses to accommodate embryonic growth and placentation (Cha et al., 2012; Dey et al., 2004). We asked whether PDZ formation is disturbed in mice with aberrant *Wnt5a* expression. Histology of cross-sections of day 6 ISs showed atypical implantation with embryos implanted close to the M pole rather than the AM pole (Figure 2A). Abnormal PDZ development was associated with atypical distribution of cytokeratin 8 (CK8), E-cadherin, and ZO-1. ZO-1 distribution was reduced with retention of CK8/E-cadherin in the LE of *Wnt5a*$^{d/d}$ and *Wnt5a*^{GOF} uteri, suggesting poor trophoblast penetration through the LE (Figure 2B). Notably, the PDZ was absent in some ISs, with the embryo entrapped within the lumen with intact LE (Figure 2B). These results suggest that disturbances in peri-implantation Wnt5a signaling contribute to abnormal PDZ formation.

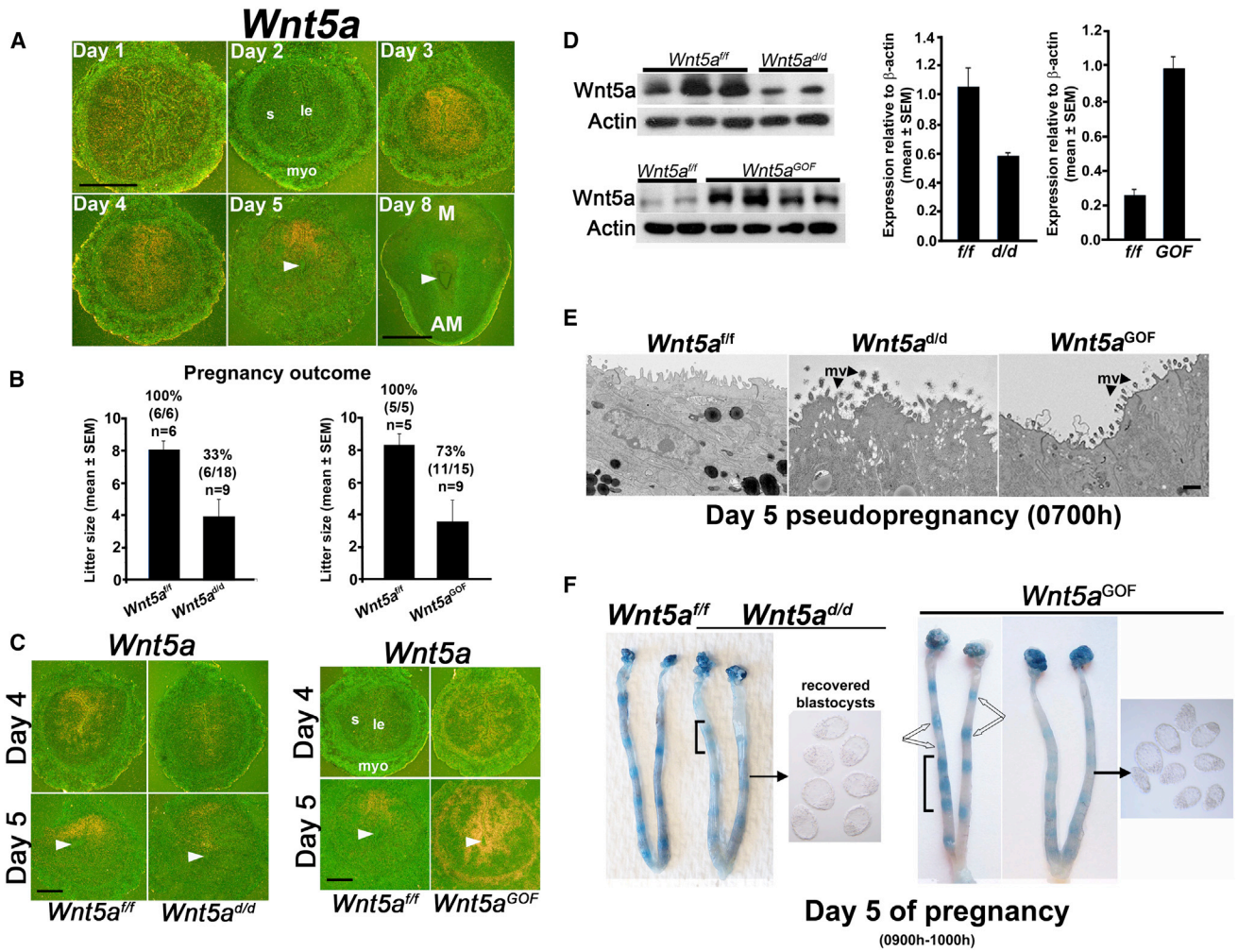

Figure 1. *Wnt5a* Is Expressed in the Peri-implantation Uterus, and Its Dysregulation Results in Defective Implantation

(A) In situ hybridization of *Wnt5a* expression patterns on days 1–5 and 8 of pregnancy. Arrowheads point to embryo location. Scale bars, 500 μm (days 1–5) and 1 mm (day 8). M, mesometrial pole; AM, antimesometrial pole.

(B) Litter sizes in pregnant *Wnt5a*$^{d/d}$ and *Wnt5a*^{GOF} females and their *Wnt5a*$^{f/f}$ littermates (mean ± SEM). Percentages and numbers within parentheses indicate the number of litters born compared to the total number of plug-positive females in each genotype. n, number of mice.

(C) In situ hybridization of uterine *Wnt5a* expression in *Wnt5a*$^{d/d}$, *Wnt5a*^{GOF}, and floxed littermates on days 4 and 5. Arrowheads point to embryo location. Scale bars, 250 μm.

(D) Western blotting of uterine Wnt5a levels of *Wnt5a*$^{d/d}$, *Wnt5a*^{GOF}, and ISs of floxed littermates on day 5. Bar diagram shows quantification of Wnt5a protein levels relative to actin (mean ± SEM).

(E) Representative transmission EM images of the apical surface of uterine LE of *Wnt5a*$^{d/d}$, *Wnt5a*^{GOF}, and floxed littermates on the morning of day 5. mv, microvilli. Scale bar, 500 nm.

(F) Day 5 ISs (blue bands) in *Wnt5a*$^{d/d}$ and *Wnt5a*^{GOF} females. Unfilled arrows indicate differential blue band intensities in adjacent ISs. Brackets indicate clustering of ISs. Unattached blastocysts retrieved from uterine luminal flushings from representative mice are shown.

s, stroma; myo, myometrium.

Implantation Sites in *Wnt5a*$^{d/d}$ and *Wnt5a*^{GOF} Mice Show Aberrant M-AM Orientation

To gain further insight in decidualization under dysregulated Wnt5a levels, we assessed decidual growth on day 8. We found abnormal embryo spacing and different sizes of ISs in *Wnt5a*$^{d/d}$ and *Wnt5a*^{GOF} females (Figure 2C), indicating asynchronous development. Furthermore, *Wnt5a*$^{d/d}$ ISs assumed a more spherical morphology with reduced cyclooxygenase 2 (Cox2) expression in contrast to the elliptical appearance in floxed littermates with appropriate M-AM axis formation and Cox2 expression at the M pole (Figure 2D). Thus, appropriate M-AM orientation in *Wnt5a*$^{d/d}$ ISs was not realized. Ratios of the length along the M-AM axis respective to the anterior-posterior (A-P) axis in *Wnt5a*$^{d/d}$ ISs were ~25% smaller than *Wnt5a*$^{f/f}$ sites (Figure S2A). Similar phenotypes were noted in *Wnt5a*^{GOF} females (Figures 2C and S2A). Because Wnt5a levels are normally low from day 8 onward, we attribute these defects to adverse effects originating at the time of implantation. In several *Wnt5a*$^{d/d}$ and *Wnt5a*^{GOF}

females, some decidual growth was noted on day 8 even with inappropriate M-AM orientation of ISs (Figures 2C and S2A). This observation resembles the results of previous studies that decidualization initiated from aberrant implantation can persist for a limited time (Song et al., 2002; Sun et al., 2012).

Wnt5a$^{d/d}$ and *Wnt5a*^{GOF} Females Show Increased Resorption Rates

We speculated that early defects would lead to abnormalities at later stages. Indeed, increasing numbers of resorption sites on days 10 and 12 were noted in *Wnt5a*-dysregulated females (Figures 2E–2G). Placental development was disrupted, and embryos were substantially smaller or absent in many ISs from day 10 onward. On day 10, the trophoblast giant cell (TGC) layer, as marked by *Prl3d1* expression, normally lies between the maternal decidua basalis and developing placenta. However, clusters of *Prl3d1*-positive TGCs were present in *Wnt5a*$^{d/d}$ and *Wnt5a*^{GOF} ISs in lieu of the embryo proper (Figure S2B). ISs that contained placentae had smaller spongiotrophoblast compartments as indicated by reduced *Tpbpa* expression (Figure S2B). Many *Wnt5a*$^{d/d}$ and *Wnt5a*^{GOF} ISs underwent resorption by day 12, but those few ISs that persisted showed abnormal placentation (Figure S2C). *Gcm1*-positive syncytiotrophoblasts in the labyrinth failed to elongate, suggesting disrupted secondary branching morphogenesis of placental villi (Figure S2C). In summary, both *Wnt5a*$^{d/d}$ and *Wnt5a*^{GOF} mice showed more or less similar phenotypes, suggesting that regulated Wnt5a levels are critical for normal implantation, embryo spacing, decidualization, and placentation.

Expression of Uterine Receptivity Marker Genes Is Not Altered under Dysregulated Wnt5a Levels

To examine Wnt5a's role in uterine receptivity, we examined the expression of estrogen- and progesterone (P_4)-responsive markers of uterine receptivity in *Wnt5a*$^{d/d}$ and *Wnt5a*^{GOF} mice on day 4 (day of receptivity) (Lee et al., 2006; Lim et al., 1997; Matsumoto et al., 2002; Song et al., 2000; Stewart et al., 1992). Expression patterns of P_4-responsive genes *Hoxa10* and *Ihh* in stromal and epithelial cells, respectively, and estrogen-responsive gene *Lif* in glandular epithelial cells in *Wnt5a*$^{d/d}$ and *Wnt5a*^{GOF} mice were similar to those in floxed uteri (Figures S3A and S3B). Expression of *Msx1*, another uterine receptivity marker (Daikoku et al., 2011), was also comparable in these females (Figures S3A–S3C). In addition, apicobasal polarity of LE as seen by immunofluorescence (IF) of α protein kinase C and ZO1 was comparable (Figure S3D). Uterine receptivity is characterized by differentiation of LE with increased stromal cell proliferation. We found that the population of Ki67-positive cells in the LE and stroma of *Wnt5a*$^{d/d}$ and *Wnt5a*^{GOF} females was nearly comparable to that of floxed littermates on day 4 (Figure S3E). These results suggest that defective attachment and implantation seen in *Wnt5a*$^{d/d}$ and *Wnt5a*^{GOF} mice are not due to defects in uterine receptivity on the morning of day 4. *Wnt11*, another noncanonical ligand and modestly expressed in the LE, was not altered in *Wnt5a*$^{d/d}$ or *Wnt5a*^{GOF} day 4 uteri (Figure S3F). Expression of *Wnt7a*, reported to be critical for uterine gland formation (Dunlap et al., 2011), was also similar in *Wnt5a*$^{d/d}$ and *Wnt5a*^{GOF} mice with no apparent defects in gland formation (Figure S3F). These results suggest that uterine *Wnt11* and *Wnt7a* expression does not respond to fluctuating uterine Wnt5a levels and may not intersect with uterine Wnt5a signaling.

Wnt5a$^{d/d}$ and *Wnt5a*^{GOF} Females Display Aberrant Crypt Formation and *Hbegf* Expression prior to Blastocyst Attachment

In mice, blastocysts normally implant within specialized crypts at the AM pole (Daikoku et al., 2011; Kirby, 1971). Our observation that blastocysts implanted closer to the M pole in *Wnt5a*$^{d/d}$ and *Wnt5a*^{GOF} mice on days 5 and 6 suggested that blastocyst attachment failed to occur toward the AM pole (Figures 2A and S1F). In support of this, we performed histological analysis of longitudinal uterine sections on the evening of day 4 prior to blastocyst attachment with appropriate orientation of the M-AM axis confirmed by the positioning of glands at the AM pole. We found that regularly spaced villi-like epithelial projections extended from the primary uterine lumen into the stroma toward the AM pole on the evening of day 4 in floxed females (Figure 3A). In contrast, these projections were randomly oriented in both M and AM directions in *Wnt5a*$^{d/d}$ females, with the presence of glands even at the M pole. Furthermore, crypt formation was frequently absent in these females with blastocysts situated near the M pole (Figure 3A). *Wnt5a*^{GOF} mice also showed defects in crypt formation and embryo placement, including blastocysts situated within the primary lumen rather than in a crypt or two embryos closely apposed within one site (Figure 3A). Intriguingly, directional villi-like projections toward the AM pole in floxed mice were not seen on day 3 but became evident on day 4, coincident with the initiation of a *Wnt5a* expression gradient along the M-AM axis in longitudinal sections (Figures 3B and S4A). The loss of the Wnt5a gradient is consistent with our observations of aberrant embryo spacing and crowding on day 5 under dysregulated uterine Wnt5a levels (Figure 1F).

The altered LE architecture in these mice led us to hypothesize that on-time embryo-uterine interactions were disturbed. *Hbegf* is first expressed in the LE around the blastocyst several hours before the attachment reaction and is the first known molecular link mediating blastocyst-uterine interactions in a juxtacrine and paracrine fashion (Das et al., 1994). We found that *Hbegf* expression was undetectable in the LE around the misplaced blastocyst in *Wnt5a*$^{d/d}$ or *Wnt5a*^{GOF} uteri on the evening of day 4 (Figure 3C), suggesting that the bidirectional communication was not realized under aberrant *Wnt5a* signaling.

Wnt5a$^{d/d}$ and *Wnt5a*^{GOF} Mice Have Normal Ovarian Function

Because *Pgr*^{Cre} is also expressed in ovary, we examined whether infertility/subfertility in *Wnt5a*$^{d/d}$ and *Wnt5a*^{GOF} females is due to ovarian dysfunction. *Wnt5a* is mainly expressed in corpora lutea. Its expression was slightly lower in *Wnt5a*$^{d/d}$ ovaries but higher in *Wnt5a*^{GOF} ovaries (Figure S4B), although quantitative PCR results showed no significant changes in transcript levels in these ovaries (Figure S4C). More importantly, we assessed ovarian function with respect to ovulation, fertilization, preimplantation embryo development, and hormone production. The number of ISs plus recovered blastocysts in *Wnt5a*$^{d/d}$ and *Wnt5a*^{GOF} females on day 5 was comparable to the number of

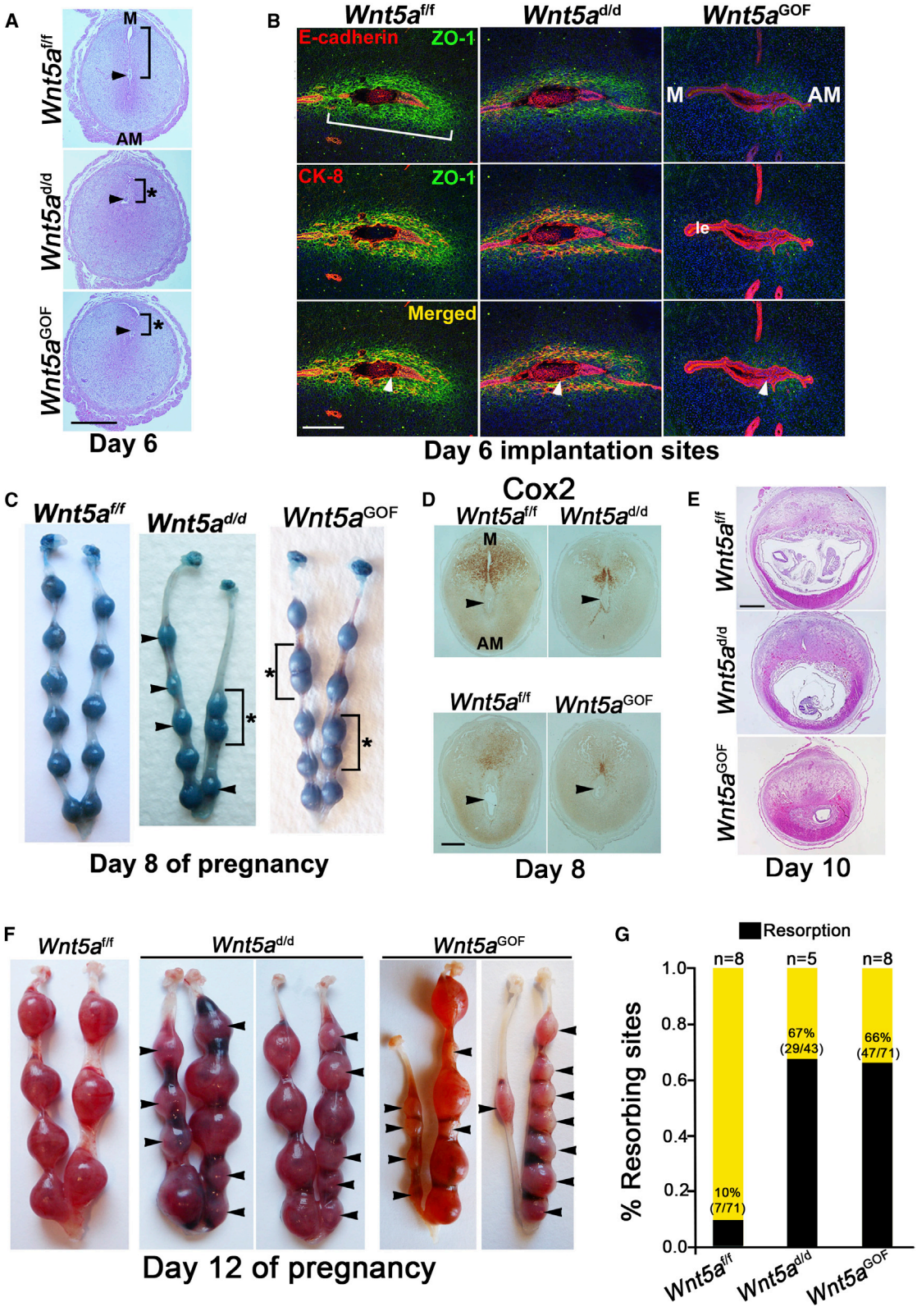

Figure 2. Defective Implantation under Dysregulated Wnt5a Levels Leads to Compromised Decidualization and Resorption

(A) Histology of day 6 ISs in *Wnt5a*$^{f/f}$, *Wnt5a*$^{d/d}$, and *Wnt5a*^{GOF} females. Brackets indicate the distance from the implanting embryo to the main LE at the M pole; asterisks indicate aberrantly short distance. Scale bar, 500 μm.

(legend continued on next page)

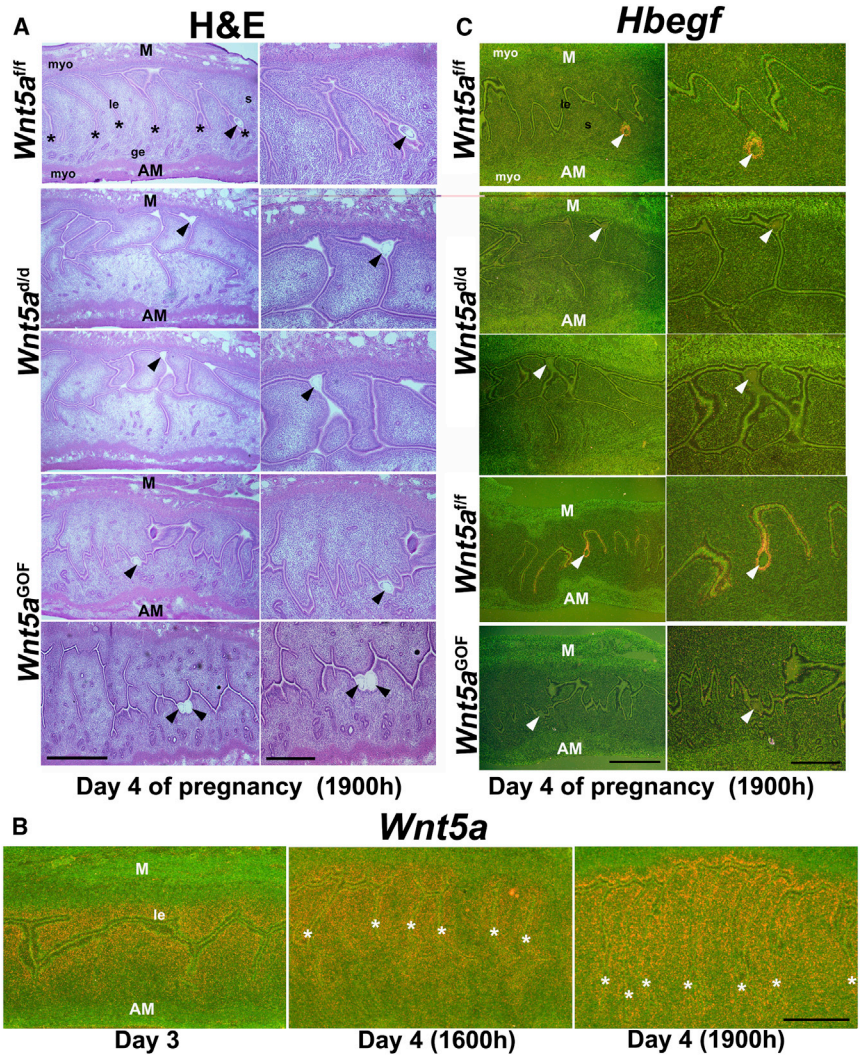

Figure 3. *Wnt5a*$^{d/d}$ and *Wnt5a*^{GOF} Females Show Poor Crypt Formation with Undetectable *Hbegf* Expression

(A) Histology of longitudinal sections of *Wnt5a*$^{d/d}$ and *Wnt5a*^{GOF} uteri approaching attachment reaction (day 4, 19:00 hr) shows aberrant luminal architecture and villi-like epithelial projections in both M and AM directions compared to regularly spaced projections toward the AM pole in floxed littermates (asterisks). Note the normal placement of blastocyst within a crypt (nidus) at the AM pole in floxed mice (top, first panel). In *Wnt5a*$^{d/d}$ and *Wnt5a*^{GOF} females, blastocysts were often situated at the M pole (second and third panels), within the primary lumen (fourth panel), and/or adjoined together within one site (bottom, fifth panel). Scale bars, 500 μm (left panels) and 250 μm (right panels).

(B) In situ hybridization of *Wnt5a* expression in WT females on day 3 (10:00 hr) and day 4 (16:00 and 19:00 hr). Asterisks indicate locations of epithelial projections toward the AM pole. Scale bar, 500 μm.

(C) In situ hybridization of *Hbegf* expression in *Wnt5a*$^{d/d}$ and *Wnt5a*^{GOF} females. Scale bars, 500 μm (left panels) and 250 μm (right panels).

Arrowheads point to the location of blastocysts. ge, glandular epithelium; s, stroma; myo, myometrium.

blue bands in floxed littermates (Figure S4D), providing evidence that these processes were comparable among these three genotypes. Serum levels of estradiol-17β (E_2) and P_4 on days 4, 8, and 12 of pregnancy in *Wnt5a*$^{d/d}$ and *Wnt5a*^{GOF} females were comparable to their floxed counterparts (Figures S4E and S4F). These results suggest normal ovarian function and hormonal milieu in *Wnt5a*$^{d/d}$ and *Wnt5a*^{GOF} females.

Uterine Wnt5a Promotes ROR2 Phosphorylation

Wnt5a can bind to ROR receptors to mediate noncanonical Wnt signaling (Green et al., 2008; Grumolato et al., 2010; Minami et al., 2010; Niehrs, 2012). ROR2 levels were upregulated in *Wnt5a*$^{d/d}$ uteri but downregulated in *Wnt5a*^{GOF} uteri; ROR1 levels did not show a similar pattern (Figure 4A). This observation suggests that Wnt5a and ROR2 interact. ROR2 was primarily localized in epithelia of floxed uteri with seemingly higher intensity in *Wnt5a*$^{d/d}$ mice on day 4, although some signals were noted in the underlying stroma (Figure S5A). This result corroborates enriched ROR2 levels in isolated primary uterine epithelial cells compared to stromal cells (Figure S5B). ROR1 was also enriched in epithelial cells rather than stromal cells (Figure S5B).

These results led us to explore if ROR2 responds to Wnt5a stimulation. Wnt5a can modulate ROR2 receptor function via tyrosine kinase activity and ROR2 autophosphorylation (Mikels et al., 2009). Immunoprecipitation (IP)-kinase assay in a uterine epithelial cell line expressing ROR2 showed that ROR2 undergoes tyrosine phosphorylation after Wnt5a stimulation (Figure 4B). IP assays also showed increased tyrosine phosphorylation of ROR2 in *Wnt5a*^{GOF} uterine extracts (Figure 4C). Furthermore, gel shift assays for ROR1 and ROR2

(B) IF of ZO-1 shows epithelioid cells in the PDZ (bracket) on day 6. E-cadherin IF marks the embryo and LE. Scale bar, 200 μm.
(C) Day 8 *Wnt5a*$^{d/d}$ and *Wnt5a*^{GOF} ISs after intravenous blue dye injection. Note differential sizes (arrowheads) and crowding (brackets, asterisks) of ISs.
(D) Immunohistochemistry shows reduced Cox2 expression at the M pole of day 8 *Wnt5a*$^{d/d}$ and *Wnt5a*^{GOF} ISs. Scale bar, 200 μm.
(E) Histology of day 10 *Wnt5a*$^{d/d}$ and *Wnt5a*^{GOF} ISs shows resorptions. Scale bar, 1 mm.
(F) Day 12 *Wnt5a*$^{f/f}$, *Wnt5a*$^{d/d}$, and *Wnt5a*^{GOF} uterine horns.
(G) Resorption rate in *Wnt5a*$^{d/d}$ and *Wnt5a*^{GOF} females on day 12. Percentages and numbers within parentheses indicate the number of resorptions over total number of ISs.
n, number of mice. M, mesometrial pole; AM, antimesometrial pole. Arrowheads point to the location of embryos or resorption sites.

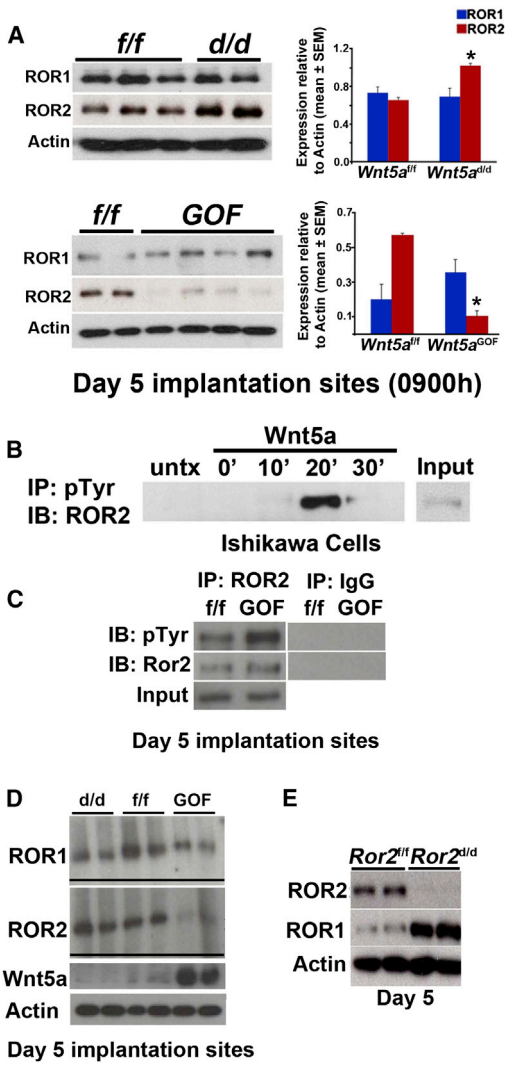

Figure 4. Uterine Wnt5a Levels Influence ROR Levels, and Uterine Inactivation of *Ror1* and *Ror2* Shows Fertility Defects

(A) Western blotting results of ROR1 and ROR2 in day 5 *Wnt5a*$^{d/d}$ and *Wnt5a*^{GOF} ISs. Bar diagram shows quantification of ROR levels (*$p < 0.05$, mean ± SEM).

(B) IP-kinase assay for ROR2 tyrosine phosphorylation in a uterine epithelial cell line (Ishikawa) exposed to Wnt5a. IB, immunoblot.

(C) IP results show increased tyrosine phosphorylation of ROR2 in day 5 ISs.

(D) Gel shift immunoblotting shows upward shift of ROR1 and ROR2 in *Wnt5a*^{GOF} sites and downward shift in *Wnt5a*$^{d/d}$ ISs on day 5.

(E) Western blotting results from *Ror2*$^{d/d}$ day 5 ISs show compensation by ROR1 for ROR2 deficiency.

phosphorylation showed downward and upward shifts in day 5 uterine extracts of *Wnt5a*$^{d/d}$ and *Wnt5a*^{GOF} females, respectively (Figure 4D). These results intrigued us to determine the significance of ROR1 and ROR2 in female fertility.

Mice with Uterine Deletion of Both *Ror1* and *Ror2* Show Severe Subfertility

We first examined if uterine inactivation of ROR2 (*Ror2*$^{d/d}$) in mice has adverse effects on fertility. Despite efficient depletion of ROR2 (Figure 4E), *Ror2*$^{d/d}$ females had normal fertility (Figure 5A). We speculated that ROR1 compensated for ROR2 deficiency because of their redundant functions (Ho et al., 2012; Lyashenko et al., 2010; Nomi et al., 2001). Indeed, *Ror2*$^{d/d}$ uteri had increased levels of ROR1 (Figure 4E). Females with uterine deletion of *Ror1* showed normal fertility: *Ror1*$^{d/d}$, 8.50 ± 0.56 pups/litter (n = 6); *Ror1*$^{f/f}$, 9.0 ± 0.81 (n = 6). Mice with uterine deletion of both alleles of *Ror1* and one allele of *Ror2* also had fertility comparable to floxed littermates (*Ror1*$^{d/d}$ *Ror2*$^{d/+}$, 7.0 ± 1.0 pups/litter [n = 3]; *Ror1*$^{f/f}$*Ror2*$^{f/f}$, 8.17 ± 0.48 [n = 6]; mean ± SEM), suggesting that one allele of uterine *Ror2* is sufficient for normal fertility. We then examined fertility in mice with uterine deletion of both alleles of *Ror1* and *Ror2* (*Ror1*$^{d/d}$*Ror2*$^{d/d}$). *Ror1*$^{d/d}$*Ror2*$^{d/d}$ females showed severe subfertility with only 29% of plug-positive females producing a small number of pups (Figure 5B) and high resorption rates on day 12 (Figures 5C and 5D).

On day 5, defective implantation was marked by very weak or an absence of blue bands in *Ror1*$^{d/d}$*Ror2*$^{d/d}$ uteri with efficient deletion of both genes (Figures 5E and 5F); unattached blastocysts were recovered from these mice. Again, we found defective crypt formation with embryos entrapped within the highly branched LE on the evening of day 4 prior to blastocyst attachment (Figure 5G). These findings suggest that blastocyst attachment was defective, leading to late-stage defects. Defective implantation seemingly did not result from aberrant expression of uterine receptivity genes *Lif* or *Ihh*; their expression was normal (Figures S5C and S5D). Ovarian levels of ROR1 or ROR2 and serum P_4 and E_2 levels were also comparable between *Ror1*$^{f/f}$*Ror2*$^{f/f}$ and *Ror1*$^{d/d}$*Ror2*$^{d/d}$ females (Figures S5E and S5F), suggesting normal ovarian function and responsiveness.

On day 6, the formation of the PDZ as determined by histology and localization of ZO-1/CK8 showed embryos entrapped within the intact LE (Figures S5G and S5H). These changes are strikingly similar to those observed in females with dysregulated Wnt5a signaling, thus reinforcing the critical role of Wnt5a-ROR signaling in blastocyst attachment, implantation, and decidualization.

Wnt5a-ROR Signaling Influences *Bmp2* Signaling during Implantation

Normally, *Bmp2* is expressed in the stroma surrounding the blastocyst at the initiation of implantation and markedly increases in decidualization. Because Bmp2 is critical for these events (Lee et al., 2007; Paria et al., 2001), we assessed uterine *Bmp2* expression in *Wnt5a*$^{d/d}$ and *Wnt5a*^{GOF} females. We found reduced *Bmp2* expression at the ISs of these mice on day 5 with attenuated nuclear localization of pSmad1/pSmad5/pSmad8 (Figures 5H and 5I). Bmp2 signaling is mediated by phosphorylation of Smad proteins, and Wnt5a was shown to intersect with Smad signaling in other systems (Miyoshi et al., 2012). These results suggest that Bmp2 signaling is compromised with altered Wnt5a levels. In contrast, *Ptgs2* (encoding Cox2) expression, which is normally expressed both in the LE and subepithelial stroma at the ISs and critical for implantation (Lim et al., 1997), was comparable among *Wnt5a*$^{f/f}$, *Wnt5a*$^{d/d}$, *Wnt5a*^{GOF}, and *Ror1*$^{d/d}$*Ror2*$^{d/d}$ females (Figures 5H and 5I).

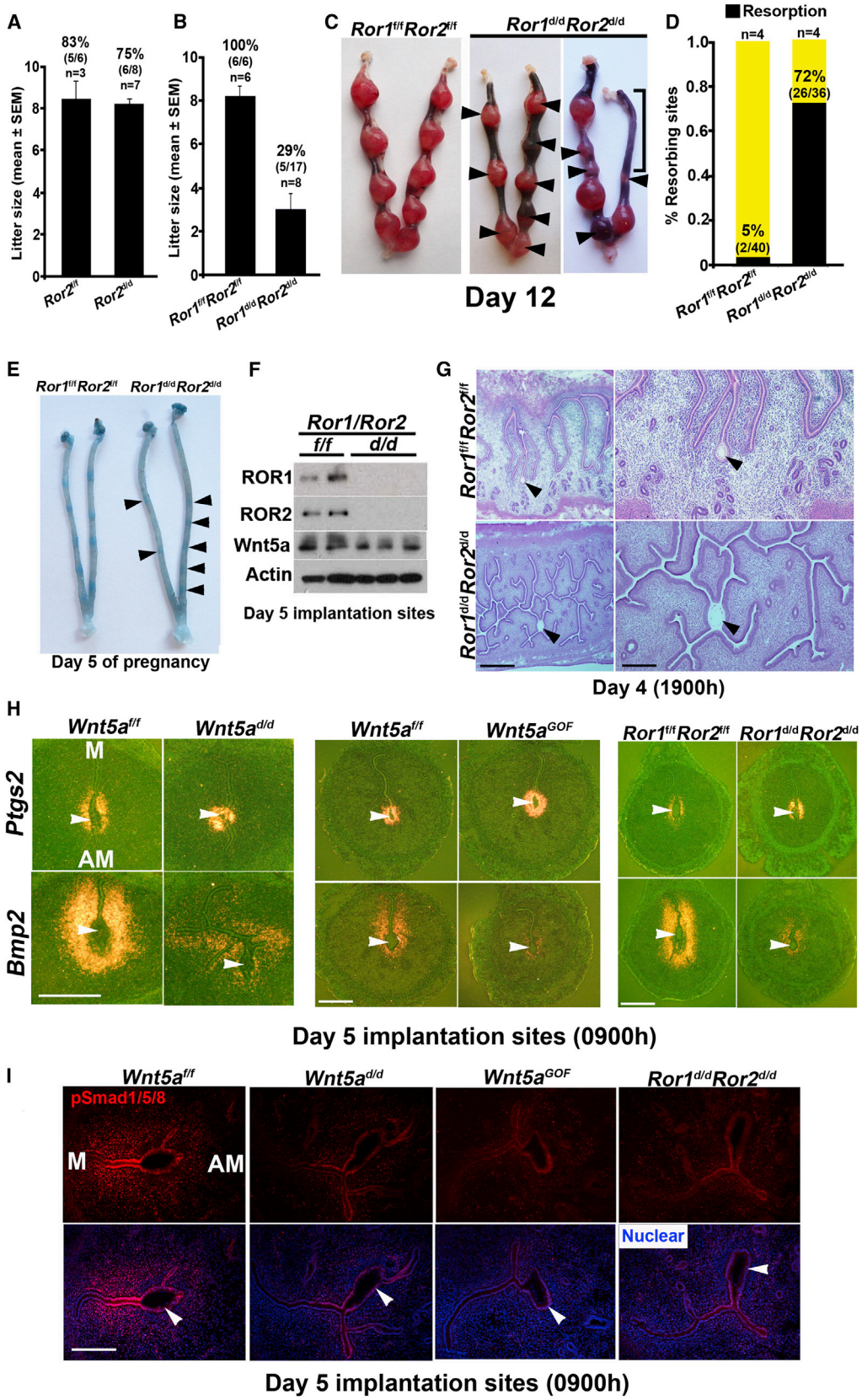

(legend on next page)

These results suggest that specific signaling pathways are affected under altered Wnt5a-ROR signaling.

DISCUSSION

This study provides evidence for the requirement of Wnt5a-ROR signaling in promoting villi-like epithelial projections toward the AM pole for crypt formation and implantation. Although the presence of crypts was noted in uterine cross-sections in mice (Daikoku et al., 2011; Kirby, 1971), the underlying mechanism regulating the formation of regularly spaced villi-like epithelial projections from the main uterine lumen to form crypts at the AM pole remained unknown. Wnt5a-ROR signaling has been reported to influence tissue patterning, cell polarity, and directional cell movement during organogenesis (Angers and Moon, 2009; Bayly and Axelrod, 2011). Our findings that Wnt5a-ROR signaling is active in the adult uterus to confer appropriate LE organization for implantation and that dysregulation of this pathway leads to aberrant crypt formation and subfertility reveal an unrecognized critical event in implantation.

Defective implantation and severe subfertility in both *Wnt5a*$^{d/d}$ and *Wnt5a*^{GOF} mice suggest that regulated Wnt5a levels are critical for early pregnancy events. Localized *Wnt5a* expression at the M pole prior to and following implantation suggests the presence of a Wnt5a gradient that directs uterine decidual growth patterning along the M-AM axis, conferring an elliptical shape and proper embryonic growth. Appropriate directional decidua formation is essential for normal embryonic growth and placentation. Our results suggest that aberrant Wnt5a-ROR signaling leads to abnormal decidual growth.

One major function of the decidua is to regulate trophoblast invasion into the stroma to direct placentation at the M pole. Our finding of defective implantation and decidual growth restriction under aberrant uterine Wnt5a levels suggests that some decidualization could be initiated, but not sustained, to support placentation and term pregnancy. This explains the abnormal placentation seen on day 10 onward in females with dysregulated Wnt5a-ROR signaling. Notably, *Wnt5a* expression is appreciably lower during decidualization in floxed females, suggesting that this defect originated from aberrations in the implantation process. This resembles previous work by us and others (Song et al., 2002; Sun et al., 2012; Ye et al., 2005).

The epithelial-mesenchymal interaction during implantation constitutes a reciprocal signaling circuitry between the LE and stroma. Our study suggests that regulated Wnt5a-ROR2 signaling participates in this transition. Reduced *Bmp2* and pSMAD1/pSmad5/pSmad8 expression with disrupted PDZ formation under aberrant Wnt5a-ROR signaling suggests that this pathway influences Bmp2 signaling critical for decidualization (Lee et al., 2007). Alternatively, the defective LE architecture, conferring poor blastocyst attachment under abnormal Wnt5a-ROR signaling, perhaps resulted in defective decidualization and *Bmp2* signaling. This is a possibility because LE architecture had already become aberrant on the evening of day 4 preceding *Bmp2* expression. These results indicate a relationship among Wnt5a-ROR signaling, appropriate LE architecture, and *Bmp2* signaling for implantation and decidualization. In this context, Wnt5a was shown to aid in intestinal stem cell niche regeneration after injury via BMP-Smad signaling (Miyoshi et al., 2012).

Wnt5a-ROR signaling is active in embryogenesis (Ho et al., 2012; Yamaguchi et al., 1999). However, subfertility phenotypes in *Wnt5a*$^{d/d}$ or *Wnt5a*^{GOF} females in our studies did not stem from embryogenesis defects because females were mated with WT males. Furthermore, uterine deletion of *Ror1*/*Ror2* resulted in similar fertility defects seen in mice with dysregulated uterine Wnt5a levels, suggesting that the defects primarily originated from uterine aberrations. This is further reinforced by similar changes in LE morphology in mice with dysregulated Wnt5a or *Ror1*/*Ror2* levels. Because ovulation, fertilization, and preimplantation embryo development were not disturbed with comparable levels of E_2 and P_4 under these experimental conditions, we believe that ovarian dysfunction did not contribute to fertility defects in these mice.

In WT females, invariable orientation of villous-like epithelial projections from the primary lumen toward the AM pole with regular spacing is reminiscent of the patterning effect of planar cell polarity (PCP) signaling in organogenesis. Whether Wnt5a-ROR signaling involves PCP signaling would require functional studies using mice with conditional uterine deletion of PCP components.

Although certain aspects of implantation are similar in mice and humans, there are species-specific differences. Nonetheless, placentation in both mice and humans is hemochorial. Regarding the relevance of embryo spacing, abnormal implantation can occur close to or on the cervix in placenta previa, which causes extensive bleeding with increased mortality and/or morbidity of the mother and fetus. Aberrant embryo spacing can also contribute to complications in multiple gestation pregnancy. Because Wnt signaling is highly conserved across species, it would be interesting to know whether Wnt5a-ROR signaling is involved in human implantation.

Figure 5. Implantation Phenotype in *Ror1*$^{d/d}$*Ror2*$^{d/d}$ Females Resembles that of *Wnt5a*$^{d/d}$ Females

(A and B) Fertility of mice with uterine inactivation of *Ror2* (*Ror2*$^{d/d}$) (A) or both *Ror1* and *Ror2* (*Ror1*$^{d/d}$*Ror2*$^{d/d}$) (B) and their floxed littermates (litter size, mean ± SEM). Percentages and numbers within parentheses indicate the number of litters over total number of plug-positive females within each genotype.

(C) Day 12 *Ror1*$^{d/d}$*Ror2*$^{d/d}$ uteri. Arrowheads point to resorption sites. Bracket indicates large area of resorption.

(D) Resorption rate on day 12 in *Ror1*$^{d/d}$*Ror2*$^{d/d}$ females. Percentages and numbers within parentheses indicate the number of resorptions over total number of ISs. n, numbers of females.

(E) *Ror1*$^{d/d}$*Ror2*$^{d/d}$ ISs on day 5 after blue dye injection. Arrowheads point to locations of very weak blue bands in *Ror1*$^{d/d}$*Ror2*$^{d/d}$ females.

(F) Western blotting results of day 5 *Ror1*$^{d/d}$*Ror2*$^{d/d}$ ISs show efficient deletion of both *Ror1* and *Ror2*.

(G) Histology of the irregular LE projections of *Ror1*$^{d/d}$*Ror2*$^{d/d}$ females on day 4 (19:00 hr). Note the location of a blastocyst within a highly branched lumen. Scale bars, 500 μm (left panel) and 200 μm (right panel).

(H) In situ hybridization of *Ptgs2* and *Bmp2* in *Wnt5a*$^{d/d}$, *Wnt5a*^{GOF}, and *Ror1*$^{d/d}$*Ror2*$^{d/d}$ ISs on day 5. Scale bars, 500 μm.

(I) IF results for phospho-Smad1/Smad5/Smad8 (pSmad1/pSmad5/pSmad8) in *Wnt5a*$^{d/d}$, *Wnt5a*^{GOF}, and *Ror1*$^{d/d}$*Ror2*$^{d/d}$ day 5 ISs. Scale bar, 100 μm. Arrowheads point to locations of blastocysts.

Collectively, our studies show that altered Wnt5a-ROR signaling leads to defects prior to and during blastocyst attachment, poor decidual growth, placentation, and pregnancy outcome. This study has revealed a critical role for Wnt5a-ROR signaling in LE remodeling for blastocyst attachment and implantation and has expanded our understanding of implantation biology.

EXPERIMENTAL PROCEDURES

For detailed methods, see Supplemental Experimental Procedures.

Mice

Pgr$^{Cre/+}$, *Wnt5a*$^{loxP/loxP}$, and/or *Ror1*$^{loxP/loxP}$/*Ror2*$^{loxP/loxP}$ floxed lines were generated as described (Ho et al., 2012; Miyoshi et al., 2012; Soyal et al., 2005). Details of *Wnt5a* overexpressing floxed mouse line generation are described in Supplemental Experimental Procedures. *Wnt5a*$^{d/d}$, *Wnt5a*^{GOF}, and *Ror1*$^{d/d}$*Ror2*$^{d/d}$ mice were generated by mating floxed females with *Pgr*$^{Cre/+}$ males, as described by Daikoku et al. (2011). All mice used in this study were housed in the Cincinnati Children's Animal Care Facility according to NIH and institutional guidelines for the use of laboratory animals. All protocols were approved by the Institutional Animal Care and Use Committee.

Analysis of Pregnancy Events

Ovulation, fertilization, preimplantation embryo development, and implantation were assessed as described by Daikoku et al. (2011).

Immunostaining and Histology

Tissue sections from control and experimental groups were processed onto the same slide for immunohistochemistry and IF (Daikoku et al., 2011).

RNA Isolation and qRT-PCR

Quantitative RT-PCR (qRT-PCR) was performed as described by Daikoku et al. (2011).

In Situ Hybridization

Paraformaldehyde-fixed frozen sections from control and experimental groups were processed onto the same slide and hybridized with ^{35}S-labeled or digoxigenin-labeled cRNA probes (Daikoku et al., 2011; Simmons et al., 2008).

Primary Uterine Cell Culture

Primary epithelial and stromal cells were isolated and cultured with ≥95% purity as described by Daikoku et al. (2011).

Immunoblotting

Western blotting was performed as described by Daikoku et al. (2011). The same blots were used for quantitative analysis of each protein. Bands were visualized using an ECL kit (GE Healthcare). Actin served as a loading control.

Immunoprecipitation

IP was performed as described by Daikoku et al. (2011).

IP-Kinase Assay

Ishikawa cells (ATCC) expressing endogenous ROR2 were lysed and subjected to IP-kinase assay as previously described with modification (Paria et al., 1993).

Electron Microscopy

Sections (80 nm) of *Wnt5a*$^{f/f}$ and *Wnt5a*^{GOF} uteri on day 5 of pseudopregnancy were cut with a Leica UC-7 ultramicrotome, stained with 3% uranyl acetate and Sato's Lead, and examined under a JEOL JEM-1400 Transmission Electron Microscope at 80 kV.

Assay of Serum E_2 and P_4 Levels

Sera were collected on days 4, 8, and 12 of pregnancy, and E_2 and P_4 levels were measured by EIA kits (Cayman Chemical) (Daikoku et al., 2011).

Statistics

Statistical analyses were performed using two-tailed Student's t test. A value of $p < 0.05$ was considered statistically significant.

SUPPLEMENTAL INFORMATION

Supplemental Information includes Supplemental Experimental Procedures and five figures and can be found with this article online at http://dx.doi.org/10.1016/j.celrep.2014.06.027.

AUTHOR CONTRIBUTIONS

J.C., C.P., X.S., S.-W.C., R.A., H.-Y.H.H., T.P.Y., and S.K.D. designed experiments. J.C., A.B., C.P., X.S., Y.L., and R.A. performed all animal, biochemical, histological, molecular, and cell biological experiments. S.-W.C., H.-Y.H.H., R.A., and T.P.Y. provided reagents, mouse lines, and technical advice. J.C., A.B., C.P., X.S., Y.L., S.-W.C., R.A., H.-Y.H.H., T.P.Y., and S.K.D., analyzed data. J.C., C.P., X.S., H.-Y.H.H., T.P.Y., and S.K.D. wrote the manuscript.

ACKNOWLEDGMENTS

We thank Michael Greenberg (Harvard) for generously providing the *Ror1 and Ror2* floxed mice and Francesco DeMayo and John B. Lydon (Baylor) for the *Pgr-Cre* mice. The ROR2 antibody was kindly provided by Yasuhiro Minami (Kyoto) and the phospho-Smad1/Smad5/Smad8 antibody by Dan Vasiliauskas, Susan Morton, Tom Jessell, and Ed Laufer (Columbia). We are thankful to Barbara Fegley and the Electron Microscopy Research Lab (University of Kansas Medical Center) for assistance with electron microscopy experiments (9P20GM104936). This work was supported in part by grants from the NIH (HD068524 and DA06668) and March of Dimes (21-FY12-127 and 22-FY13-543) (to S.K.D.) and by the Intramural Research Program of the NIH, National Cancer Institute, Center for Cancer Research (to T.P.Y.). J.C. is a National Research Service Award fellow (F30AG040858) of the University of Cincinnati MSTP, and X.S. was supported by a Lalor Foundation Postdoctoral Fellowship.

Received: November 23, 2013
Revised: May 24, 2014
Accepted: June 17, 2014
Published: July 17, 2014

REFERENCES

Angers, S., and Moon, R.T. (2009). Proximal events in Wnt signal transduction. Nat. Rev. Mol. Cell Biol. *10*, 468–477.

Bayly, R., and Axelrod, J.D. (2011). Pointing in the right direction: new developments in the field of planar cell polarity. Nat. Rev. Genet. *12*, 385–391.

Cha, J., Sun, X., and Dey, S.K. (2012). Mechanisms of implantation: strategies for successful pregnancy. Nat. Med. *18*, 1754–1767.

Daikoku, T., Cha, J., Sun, X., Tranguch, S., Xie, H., Fujita, T., Hirota, Y., Lydon, J., DeMayo, F., Maxson, R., and Dey, S.K. (2011). Conditional deletion of Msx homeobox genes in the uterus inhibits blastocyst implantation by altering uterine receptivity. Dev. Cell *21*, 1014–1025.

Das, S.K., Wang, X.N., Paria, B.C., Damm, D., Abraham, J.A., Klagsbrun, M., Andrews, G.K., and Dey, S.K. (1994). Heparin-binding EGF-like growth factor gene is induced in the mouse uterus temporally by the blastocyst solely at the site of its apposition: a possible ligand for interaction with blastocyst EGF-receptor in implantation. Development *120*, 1071–1083.

Dey, S.K., Lim, H., Das, S.K., Reese, J., Paria, B.C., Daikoku, T., and Wang, H. (2004). Molecular cues to implantation. Endocr. Rev. *25*, 341–373.

Dunlap, K.A., Filant, J., Hayashi, K., Rucker, E.B., 3rd, Song, G., Deng, J.M., Behringer, R.R., DeMayo, F.J., Lydon, J., Jeong, J.W., and Spencer, T.E. (2011). Postnatal deletion of Wnt7a inhibits uterine gland morphogenesis and compromises adult fertility in mice. Biol. Reprod. *85*, 386–396.

Gao, B., Song, H., Bishop, K., Elliot, G., Garrett, L., English, M.A., Andre, P., Robinson, J., Sood, R., Minami, Y., et al. (2011). Wnt signaling gradients establish planar cell polarity by inducing Vangl2 phosphorylation through Ror2. Dev. Cell *20*, 163–176.

Green, J.L., Kuntz, S.G., and Sternberg, P.W. (2008). Ror receptor tyrosine kinases: orphans no more. Trends Cell Biol. *18*, 536–544.

Grumolato, L., Liu, G., Mong, P., Mudbhary, R., Biswas, R., Arroyave, R., Vijayakumar, S., Economides, A.N., and Aaronson, S.A. (2010). Canonical and noncanonical Wnts use a common mechanism to activate completely unrelated coreceptors. Genes Dev. *24*, 2517–2530.

Ho, H.Y., Susman, M.W., Bikoff, J.B., Ryu, Y.K., Jonas, A.M., Hu, L., Kuruvilla, R., and Greenberg, M.E. (2012). Wnt5a-Ror-Dishevelled signaling constitutes a core developmental pathway that controls tissue morphogenesis. Proc. Natl. Acad. Sci. USA *109*, 4044–4051.

Kikuchi, A., Yamamoto, H., Sato, A., and Matsumoto, S. (2011). New insights into the mechanism of Wnt signaling pathway activation. Int. Rev. Cell Mol. Biol. *291*, 21–71.

Kirby, D.R.S. (1971). Blastocyst-Uterine Relationship before and during Implantation. In The Biology of the Blastocyst, R.J. Blandau, ed. (Chicago: The University of Chicago Press), pp. 393–412.

Lee, K., Jeong, J., Kwak, I., Yu, C.T., Lanske, B., Soegiarto, D.W., Toftgard, R., Tsai, M.J., Tsai, S., Lydon, J.P., and DeMayo, F.J. (2006). Indian hedgehog is a major mediator of progesterone signaling in the mouse uterus. Nat. Genet. *38*, 1204–1209.

Lee, K.Y., Jeong, J.W., Wang, J., Ma, L., Martin, J.F., Tsai, S.Y., Lydon, J.P., and DeMayo, F.J. (2007). Bmp2 is critical for the murine uterine decidual response. Mol. Cell. Biol. *27*, 5468–5478.

Lim, H., Paria, B.C., Das, S.K., Dinchuk, J.E., Langenbach, R., Trzaskos, J.M., and Dey, S.K. (1997). Multiple female reproductive failures in cyclooxygenase 2-deficient mice. Cell *91*, 197–208.

Lyashenko, N., Weissenböck, M., Sharir, A., Erben, R.G., Minami, Y., and Hartmann, C. (2010). Mice lacking the orphan receptor ror1 have distinct skeletal abnormalities and are growth retarded. Dev. Dyn. *239*, 2266–2277.

MacDonald, B.T., Tamai, K., and He, X. (2009). Wnt/beta-catenin signaling: components, mechanisms, and diseases. Dev. Cell *17*, 9–26.

Macheda, M.L., Sun, W.W., Kugathasan, K., Hogan, B.M., Bower, N.I., Halford, M.M., Zhang, Y.F., Jacques, B.E., Lieschke, G.J., Dabdoub, A., and Stacker, S.A. (2012). The Wnt receptor Ryk plays a role in mammalian planar cell polarity signaling. J. Biol. Chem. *287*, 29312–29323.

Matsumoto, H., Zhao, X., Das, S.K., Hogan, B.L., and Dey, S.K. (2002). Indian hedgehog as a progesterone-responsive factor mediating epithelial-mesenchymal interactions in the mouse uterus. Dev. Biol. *245*, 280–290.

Mikels, A., Minami, Y., and Nusse, R. (2009). Ror2 receptor requires tyrosine kinase activity to mediate Wnt5A signaling. J. Biol. Chem. *284*, 30167–30176.

Minami, Y., Oishi, I., Endo, M., and Nishita, M. (2010). Ror-family receptor tyrosine kinases in noncanonical Wnt signaling: their implications in developmental morphogenesis and human diseases. Dev. Dyn. *239*, 1–15.

Miyoshi, H., Ajima, R., Luo, C.T., Yamaguchi, T.P., and Stappenbeck, T.S. (2012). Wnt5a potentiates TGF-β signaling to promote colonic crypt regeneration after tissue injury. Science *338*, 108–113.

Niehrs, C. (2012). The complex world of WNT receptor signalling. Nat. Rev. Mol. Cell Biol. *13*, 767–779.

Nomi, M., Oishi, I., Kani, S., Suzuki, H., Matsuda, T., Yoda, A., Kitamura, M., Itoh, K., Takeuchi, S., Takeda, K., et al. (2001). Loss of mRor1 enhances the heart and skeletal abnormalities in mRor2-deficient mice: redundant and pleiotropic functions of mRor1 and mRor2 receptor tyrosine kinases. Mol. Cell. Biol. *21*, 8329–8335.

Paria, B.C., Das, S.K., Andrews, G.K., and Dey, S.K. (1993). Expression of the epidermal growth factor receptor gene is regulated in mouse blastocysts during delayed implantation. Proc. Natl. Acad. Sci. USA *90*, 55–59.

Paria, B.C., Zhao, X., Das, S.K., Dey, S.K., and Yoshinaga, K. (1999). Zonula occludens-1 and E-cadherin are coordinately expressed in the mouse uterus with the initiation of implantation and decidualization. Dev. Biol. *208*, 488–501.

Paria, B.C., Ma, W., Tan, J., Raja, S., Das, S.K., Dey, S.K., and Hogan, B.L. (2001). Cellular and molecular responses of the uterus to embryo implantation can be elicited by locally applied growth factors. Proc. Natl. Acad. Sci. USA *98*, 1047–1052.

Psychoyos, A. (1973). Endocrine control of egg implantation. In Handbook of Physiology, E.G.A.R.O. Greep and S.R. Geiger, eds. (Washington, D.C.: American Physiology Society), pp. 187–215.

Schambony, A., and Wedlich, D. (2007). Wnt-5A/Ror2 regulate expression of XPAPC through an alternative noncanonical signaling pathway. Dev. Cell *12*, 779–792.

Schlafke, S., and Enders, A.C. (1975). Cellular basis of interaction between trophoblast and uterus at implantation. Biol. Reprod. *12*, 41–65.

Simmons, D.G., Rawn, S., Davies, A., Hughes, M., and Cross, J.C. (2008). Spatial and temporal expression of the 23 murine Prolactin/Placental Lactogen-related genes is not associated with their position in the locus. BMC Genomics *9*, 352.

Song, H., Lim, H., Das, S.K., Paria, B.C., and Dey, S.K. (2000). Dysregulation of EGF family of growth factors and COX-2 in the uterus during the preattachment and attachment reactions of the blastocyst with the luminal epithelium correlates with implantation failure in LIF-deficient mice. Mol. Endocrinol. *14*, 1147–1161.

Song, H., Lim, H., Paria, B.C., Matsumoto, H., Swift, L.L., Morrow, J., Bonventre, J.V., and Dey, S.K. (2002). Cytosolic phospholipase A2alpha is crucial [correction of A2alpha deficiency is crucial] for 'on-time' embryo implantation that directs subsequent development. Development *129*, 2879–2889.

Soyal, S.M., Mukherjee, A., Lee, K.Y., Li, J., Li, H., DeMayo, F.J., and Lydon, J.P. (2005). Cre-mediated recombination in cell lineages that express the progesterone receptor. Genesis *41*, 58–66.

Stewart, C.L., Kaspar, P., Brunet, L.J., Bhatt, H., Gadi, I., Köntgen, F., and Abbondanzo, S.J. (1992). Blastocyst implantation depends on maternal expression of leukaemia inhibitory factor. Nature *359*, 76–79.

Sun, X., Zhang, L., Xie, H., Wan, H., Magella, B., Whitsett, J.A., and Dey, S.K. (2012). Kruppel-like factor 5 (KLF5) is critical for conferring uterine receptivity to implantation. Proc. Natl. Acad. Sci. USA *109*, 1145–1150.

van Amerongen, R., and Nusse, R. (2009). Towards an integrated view of Wnt signaling in development. Development *136*, 3205–3214.

Veeman, M.T., Axelrod, J.D., and Moon, R.T. (2003). A second canon. Functions and mechanisms of beta-catenin-independent Wnt signaling. Dev. Cell *5*, 367–377.

Yamaguchi, T.P., Bradley, A., McMahon, A.P., and Jones, S. (1999). A Wnt5a pathway underlies outgrowth of multiple structures in the vertebrate embryo. Development *126*, 1211–1223.

Ye, X., Hama, K., Contos, J.J., Anliker, B., Inoue, A., Skinner, M.K., Suzuki, H., Amano, T., Kennedy, G., Arai, H., et al. (2005). LPA3-mediated lysophosphatidic acid signalling in embryo implantation and spacing. Nature *435*, 104–108.